SUPPORTING MATERIAL

Cohesiveness tunes assembly and morphology of FG nucleoporin domain meshworks – Implications for nuclear pore permeability

Nico B. Eisele[†‡], *Aksana A. Labokha*[‡], *Steffen Frey*[‡], *Dirk Görlich*[‡], *Ralf P. Richter*[†§¶*]

[†] Biosurfaces Unit, CIC biomaGUNE, Paseo Miramon 182, 20009 San Sebastian, Spain

[‡] Department of Cellular Logistics, Max Planck Institute for Biophysical Chemistry, Am Faßberg 11, 37077 Göttingen, Germany

[§] I2BM, Department of Molecular Chemistry, J. Fourier University, 570 Rue de la Chimie, 38041 Grenoble Cedex 9, France

[¶] Max Planck Institute for Intelligent Systems, Heisenbergstraße 3, 70569 Stuttgart, Germany

* Correspondence: rrichter@cicbiomagune.es

SUPPORTING METHODS

Quantification of mass transport limited FG domain adsorption rates. In our experimental in situ ellipsometry setup, i.e. a flat surface opposite a rotating stirrer, transport of molecules to the film can be adequately described by diffusion through an unstirred layer next to the surface (1). The mass transport limited adsorption rate of FG domains can be estimated from a reference measurement of an adsorption process that is limited by mass transport and that occurs under identical stirring conditions (1):

$$\left(\frac{\partial \Gamma}{\partial t}\right)_{\mathrm{FG}} = \left(\frac{R_{\mathrm{ref}}}{R_{\mathrm{FG}}}\right)^{2/3} \frac{[\mathrm{FG}]}{[\mathrm{ref}]} \left(\frac{\partial \Gamma}{\partial t}\right)_{\mathrm{ref}}.$$

We chose the adsorption of avidin with a concentration of 0.1 μM to a biotinylated SLB (2) as the reference and measured an adsorption rate of $(\partial\Gamma/\partial t)_{\mathrm{ref}} = 2.07 \pm 0.12\,\mathrm{pmol/cm^2/min}$ (mean ± standard deviation from three measurements). The Stokes radius for avidin is $R_{\mathrm{ref}} = 3.4\,\mathrm{nm}$, and we estimate R_{FG} to be between 3.5 and 8.7 nm, based on reported values for other FG domains (3,4) and other intrinsically disordered or chemically denatured proteins (5,6). These considerations lead to a mass transport limited adsorption rate for FG domains between 7.6 and 21.5 pmol/cm^2/min at a bulk concentration of 0.9 ± 0.1 μM. This range is represented as a gray-shaded area in Fig. 2 *a*.

SUPPORTING FIGURES

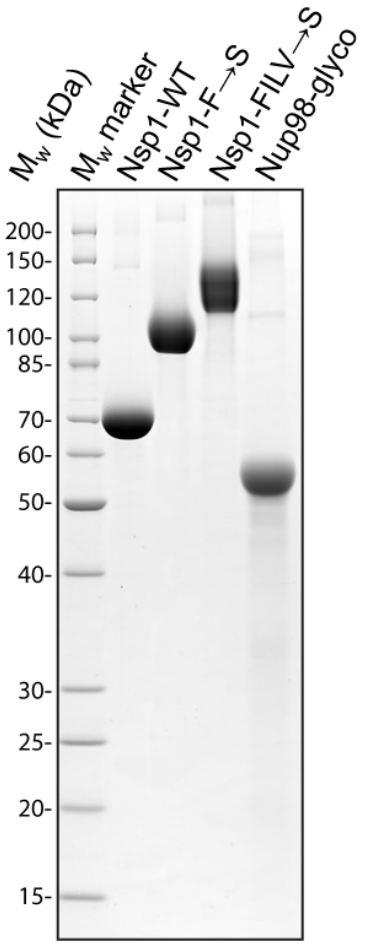

FIGURE S1: Quality of purified recombinant FG domains used in this study. FG domains with His-tag were dissolved in 30% formamide and diluted 1:10 in SDS sample buffer. 2.5 µg of each protein was resolved by SDS-PAGE and stained with Coomassie G250. All preparations contain more than 90% full length protein.

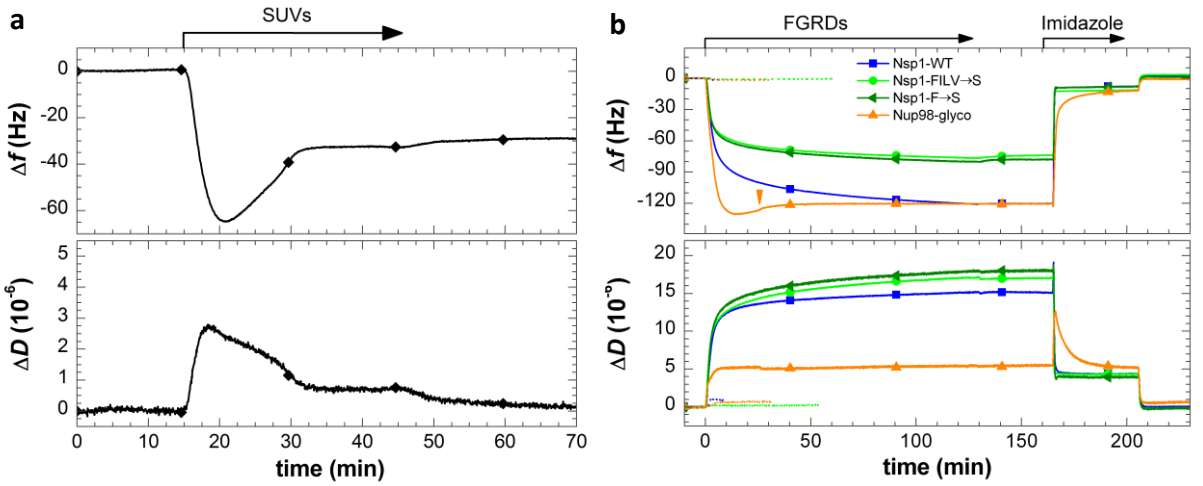

FIGURE S2: FG domains are anchored specifically and stably through their terminal His-tags to NTA-functionalized SLBs. (*a*) SLB formation monitored by QCM-D. Silica surfaces in working buffer were exposed to 50 µg/ml SUVs made of 90 mol-% DOPC and 10 mol-% bis-NTA-functionalized lipids. Start and duration of the incubation is indicated by an arrow. The two-phase behavior together with the final changes in frequency and dissipation of Δf = -28 Hz and $\Delta D < 0.3 \cdot 10^{-6}$, respectively, characterizes the formation of an SLB of good quality (7). The minor shifts in Δf and ΔD at about 44 min are due to the removal of $NiCl_2$ from the solution during rinsing in working buffer. (*b*) Formation of FG domain films was monitored by QCM-D on SLBs formed from SUVs containing either a mixture of 90 mol-% DOPC and 10 mol-% bis-NTA-functionalized lipids (*solid lines*), or only DOPC (*dotted lines*). Baselines (i.e. $\Delta f = \Delta D = 0$) correspond to the responses for bare SLBs. Start and duration of incubation steps with different samples are indicated with solid arrows on top of the plot. After each incubation step, the solution phase was replaced by working buffer. Strong changes in frequency and dissipation upon incubation with different His-tagged FG domain species (*listed in the legend*) at 45 µg/ml (i.e. 0.7 µM Nsp1-FILV→S, Nsp1-F→S and Nsp1-WT and 0.8 µM Nup98-glyco) on NTA-functionalized SLBs reflect the formation of soft and hydrated films. No changes in Δf and ΔD for Nsp1-derived FG domains and minor changes for Nup98-glyco upon rinsing in buffer (rinsing of Nup98-glyco was performed at 25 min, i.e. earlier than for the other species; *orange arrowhead*) indicate stable grafting. After exposure to 500 mM imidazole at pH 7.4, Δf and ΔD return to baseline levels, demonstrating specificity of binding. Changes in Δf and ΔD upon exchange from imidazole containing solution to pure working buffer do not reflect any changes on the surface but result from a change in the viscosity and/or density of the surrounding solution owing to the presence of imidazole. When exposed at 90 µg/ml (i.e. 1.5 µM Nsp1-FILV→S, Nsp1-F→S, and Nup98-glyco and 1.4 µM Nsp1-WT) to SLBs made of pure DOPC, none of the His-tagged FG domains induced appreciable QCM-D responses, confirming that the FG domains do not bind to SLBs that lack NTA functionality.

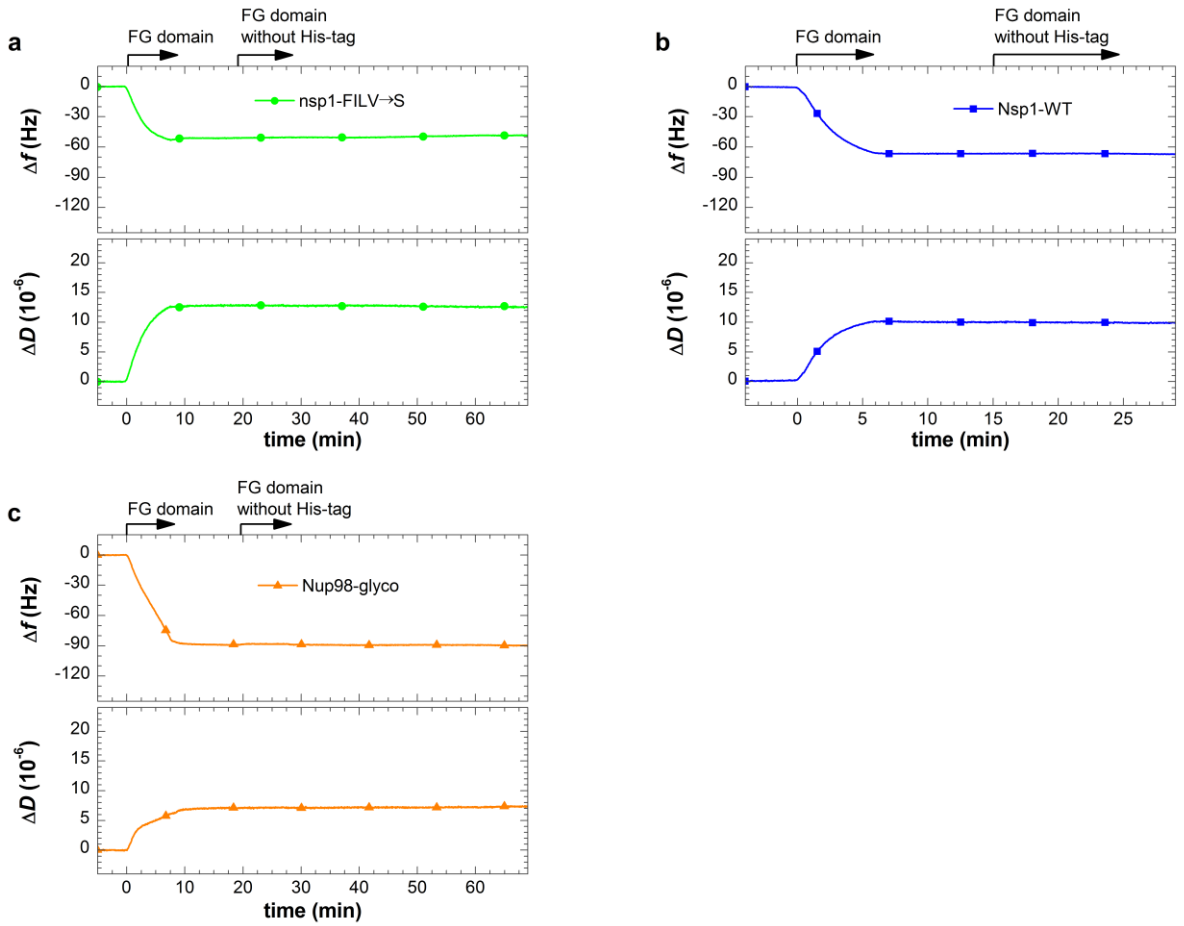

FIGURE S3: All FG domains in the films are anchored to the SLB. SLBs with 10 mol-% bis-NTA functionalized lipids were formed and incubated with His-tagged FG domains at a concentration of 23 µg/ml (0.4 µM). Incubation was interrupted, by rinsing in working buffer, when frequency shifts reached between 50 and 70 % of the maximal frequency shifts observed in Fig. S1 *b*. No changes in Δf and ΔD were observed when the films were subsequently incubated with the same FG domain types lacking the His-tags at identical concentration. We conclude that homophilic interactions or entanglements are not sufficient to entrap individual FG domains stably in the films. All stably bound FG domain molecules must hence be anchored to the SLB.

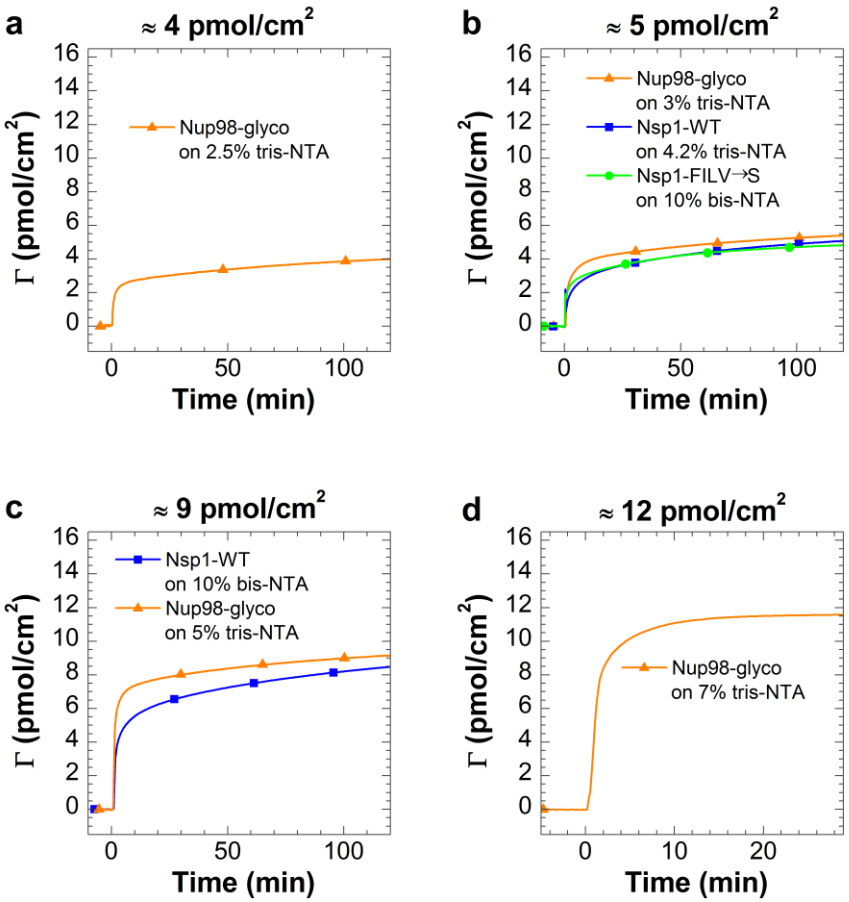

FIGURE S4: Tuning FG domain surface density. FG domain films with defined and reproducible grafting densities (*indicated on top of each plot*) were obtained by tuning the valency (*bis* or *tris*) and fraction (in mol-%) of NTA-functionalized lipids in the SUVs from which the SLBs were formed (*indicated in each plot*). FG domains were incubated at concentrations of 56 μg/ml (1.0 μM) for Nup98-glyco and 113 μg/ml (1.8 μM) for Nsp1-WT and (1.9 μM) Nsp1-FILV→S.

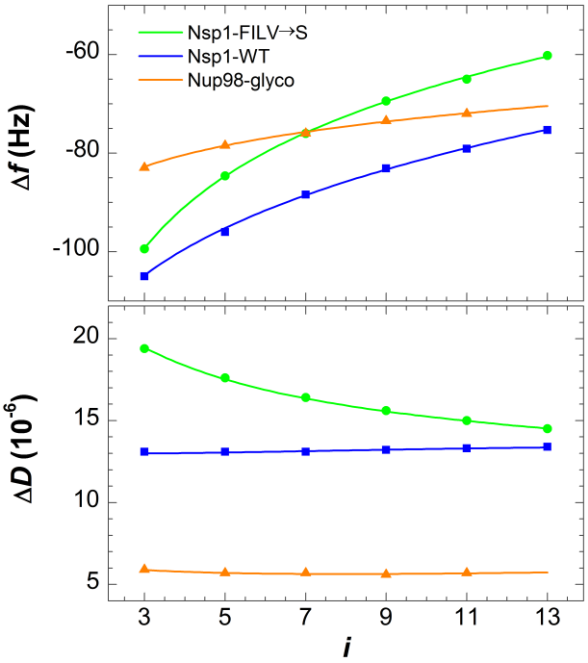

FIGURE S5: FG domain film thickness determination from QCM-D data. Film thickness was estimated by fitting the QCM-D data for all overtones to a continuum viscoelastic model (8) with the software QTM (D. Johannsmann, Technical University of Clausthal, Germany (9); option "small load approximation"), as described in detail elsewhere (10). The model relates the measured QCM-D responses, Δf and ΔD as a function of the overtone number, to the viscoelastic properties and the thickness of the surface-confined film (10,11). The figure shows the final QCM-D responses (*symbols*) for the formation of FG domain films of about 5 pmol/cm^2 (see Fig. S3 *b* for film formation conditions; FG domain type is indicated in the plot) together with the best fits (*lines*) as a function of overtone *i*. Resulting film thicknesses are shown in Fig. 3 *b*, where error bars correspond to joint confidence regions with a confidence level of one standard deviation, and were determined as described in ref. (10).

SUPPORTING REFERENCES

1. Hermens, W. T., M. Beneš, R. Richter, and H. Speijer. 2004. Effects of flow on solute exchange between fluids and supported biosurfaces. Biotechn Appl Biochem 39:277-284.
2. Bingen, P., G. Wang, N. F. Steinmetz, M. Rodahl, and R. P. Richter. 2008. Solvation effects in the QCM-D response to biomolecular adsorption - a phenomenological approach. Anal Chem 80:8880-8890.
3. Denning, D. P., S. S. Patel, V. Uversky, A. L. Fink, and M. Rexach. 2003. Disorder in the nuclear pore complex: the FG repeat regions of nucleoporins are natively unfolded. Proc Natl Acad Sci U S A 100:2450-2455.
4. Yamada, J., J. L. Phillips, S. Patel, G. Goldfien, A. Calestagne-Morelli, H. Huang, R. Reza, J. Acheson, V. V. Krishnan, S. Newsam, A. Gopinathan, E. Y. Lau, M. E. Colvin, V. N. Uversky, and M. F. Rexach. 2010. A bimodal distribution of two distinct categories of intrinsically disordered structures with separate functions in FG nucleoporins. Mol Cell Proteomics 9:2205-2224.
5. Kohn, J. E., I. S. Millett, J. Jacob, B. Zagrovic, T. M. Dillon, N. Cingel, R. S. Dothager, S. Seifert, P. Thiyagarajan, T. R. Sosnick, M. Z. Hasan, V. S. Pande, I. Ruczinski, S. Doniach, and K. W. Plaxco. 2004. Random-coil behavior and the dimensions of chemically unfolded proteins. Proc Natl Acad Sci U S A 101:12491-12496.
6. Tcherkasskaya, O., E. A. Davidson, and V. N. Uversky. 2003. Biophysical constraints for protein structure prediction. J Proteome Res 2:37-42.
7. Richter, R. P., R. Bérat, and A. R. Brisson. 2006. The formation of solid-supported lipid bilayers - an integrated view. Langmuir 22:3497-3505.
8. Domack, A., O. Prucker, J. Rühe, and D. Johannsmann. 1997. Swelling of a polymer brush probed with a quartz crystal resonator. Phys Rev E 56:680-689.
9. Johannsmann, D. http://www2.pc.tu-clausthal.de/dj/software_en.shtml.
10. Eisele, N. B., F. I. Andersson, S. Frey, and R. P. Richter. 2012. Viscoelasticity of thin biomolecular films: a case study on nucleoporin phenylalanine-glycine repeats grafted to a histidine-tag capturing QCM-D sensor. Biomacromolecules 13:2322-2332.
11. Reviakine, I., D. Johannsmann, and R. P. Richter. 2011. Hearing what you cannot see and visualizing what you hear: interpreting quartz crystal microbalance data from solvated interfaces. Anal Chem 83:8838-8848.